Dispersion in photonic media and diffraction from gratings: a different modal expansion for the R-matrix propagation technique

J. Merle Elson and P. Tran

Research and Technology Division, U.S. Naval Air Warfare Center Weapons Division, China Lake, California 93555-6001

Received November 18, 1994; revised manuscript received March 27, 1995; accepted March 29, 1995

A method of solving problems of diffraction and dispersion in electromagnetic theory is presented. A modal expansion technique is used with a recursive **R**-matrix propagation scheme. This method retains the inherent **R**-matrix numerical stability and yet, contrary to some recent studies, is quite easy to implement for periodic structures (both two and three dimensional), including gratings and photonic crystal media. Grating structures may be multilayered structure, linear or crossed. Photonic media may be latticelike structures of finite or infinite depth. The eigenvalues of the modes are obtained by diagonalizing a matrix rather than searching for zeros of characteristic equations. Diffraction from dielectric and metallic sinusoidal gratings is calculated, and the results are compared with other published results. Transmission is calculated through a seven-layer-deep square arrangement of dielectric cylinders. Also, with the Floquet theorem, the bulk dispersion of the same cylinder geometry is calculated, and the results are compared with other published results. Of particular interest as a computational tool is a description of how a complex structure can be recursively added, whole structures at a time, after the initial structure has been calculated. This is very significant in terms of time savings, since most of the numerical work is done with the initial structure.

1. INTRODUCTION

In a recent paper Li[1] applied the multilayer modal method with **R**-matrix propagation for the calculation of diffracted intensity from gratings. This method divides the grating into sublayers, and a modal expansion in each sublayer is used to obtain the **R** matrix for propagation. This **R**-matrix propagation algorithm, first described in the field of chemical physics,[2] is comparatively free of the numerical instability that exists for certain **T**-matrix propagation schemes. Unlike the **T**-matrix approach, which seeks a matrix that relates the electric and magnetic fields on one side of a layer to the electric and magnetic fields on the other side of the layer, the **R**-matrix method relates the electric field of both sides of a layer to the magnetic field on both sides. A recursive formula is derived to allow stacking up of successive layers to form a global **R** matrix for any structure of interest. The field inside each layer is expanded with Li's generalization of the classical modal method of Botten *et al.*[3] Although this method was claimed to be applicable to arbitrary profiles, it is quite cumbersome in practice. In particular, one is required to look for zeros of a characteristic equation in order to obtain the eigenvalues of the modes. In this paper we present another expansion approach that is very simple for arbitrary profiles and requires only the diagonalization of a matrix to obtain the eigenvalues. A comparison with Li's method will be presented for a sinusoidal grating.

The applicability of our method goes beyond gratings. There has been a lot of interest in photonic crystals that possess gaps in the dispersion[4–6] and there are many techniques for bulk dispersion calculation,[7–13] but a transmission calculation can play an important role. It may be desirable to limit the size of the crystal for practical applications, and a transmission calculation offers the ability to examine when the bulk limit is reached. Furthermore, the search for such structures is performed experimentally by measuring the transmissivity through several layers of crystal. Direct measurement of experimental data is a good, but not necessarily efficient, way of designing photonic crystals. It is desirable to have an efficient method to predict the transmission of finite-depth photonic crystals. Toward this goal we assume that a photonic crystal structure has N identical sections, and we describe here a bootstrapped **R**-matrix propagation scheme that can be used to facilitate greatly transmission calculations. To demonstrate the capabilities of this method, we will compare our result with experimental data for transmission through a square arrangement of cylinders seven rows deep ($N = 7$).

We also apply our results to calculation of the bulk dispersion relation of a photonic medium. The method is similar to that discussed by Pendry[14] but naturally follows from our **R**-matrix results and requires only that we find the eigenvalues of a matrix. We compare our dispersion results with those of Robertson *et al.*[15]

2. CALCULATION METHOD

A. General Formulas

In this section we describe our modal expansion, along with the **R**-matrix propagation scheme. As a basic calculation, we consider reflection and transmission through an arbitrary structure that is periodic in the $(\hat{x}, \hat{y})$ plane and of finite thickness in the $\hat{z}$ direction. Here we define this finite-thickness region as a *section*. We describe how

0740-3232/95/081765-07$06.00

we can expand on this basic calculation and thereby consider a repetitive structure in the $\hat{z}$ direction that consists of a finite number N of identical sections. This can apply to a one- or two-dimensional multilayered grating or a finite-thickness photonic medium. In the case of dispersion in bulk photonic media, $N = \infty$, and we apply the Floquet theorem. We defer discussion regarding this calculation until the end of this section.

In the calculation of reflection and transmission with regard to multilayered gratings or finite-thickness photonic media, there are three regions of interest: the homogeneous region containing the incident and reflected waves, the homogeneous region containing the transmitted wave, and the region containing the structure, which is described by a spatially variable dielectric function $\epsilon(\mathbf{r})$, where $\mathbf{r} = (x, y, z)$. For the homogeneous media the reflected and transmitted fields can be Fourier analyzed as

$$\mathbf{E}^r(\mathbf{r}) = \frac{1}{(2\pi)^2}\int \mathrm{d}^2K\, \mathbf{E}^r(\mathbf{K})\exp(i\mathbf{K}\cdot\mathbf{R})\exp(ipz), \quad (1a)$$

$$\mathbf{H}^r(\mathbf{r}) = \frac{1}{(2\pi)^2}\int \mathrm{d}^2K\, \mathbf{H}^r(\mathbf{K})\exp(i\mathbf{K}\cdot\mathbf{R})\exp(ipz), \quad (1b)$$

$$\mathbf{E}^t(\mathbf{r}) = \frac{1}{(2\pi)^2}\int \mathrm{d}^2K\, \mathbf{E}^t(\mathbf{K})\exp(i\mathbf{K}\cdot\mathbf{R})\exp(-ipz), \quad (1c)$$

$$\mathbf{H}^t(\mathbf{r}) = \frac{1}{(2\pi)^2}\int \mathrm{d}^2K\, \mathbf{H}^t(\mathbf{K})\exp(i\mathbf{K}\cdot\mathbf{R})\exp(-ipz), \quad (1d)$$

where $\mathbf{R} = (x, y)$ and $p = [\epsilon(\omega/c)^2 - K^2]^{1/2}$ is the wave number in the $\hat{z}$ direction with $\epsilon = \epsilon_r$ or ϵ_t pertaining to the permittivity in the corresponding region. For the region containing the structure we divide a section into sublayers such that, within each sublayer, we can assume that there is no z variation in the dielectric, whereas, in the x and y directions, the dielectric is spatially periodic. The field inside each sublayer can be Fourier analyzed as

$$\mathbf{E}(\mathbf{r}) = \frac{1}{(2\pi)^2}\int \mathrm{d}^2K\, \mathbf{E}(\mathbf{K}, z)\exp(i\mathbf{K}\cdot\mathbf{R}), \quad (1e)$$

$$\mathbf{H}(\mathbf{r}) = \frac{1}{(2\pi)^2}\int \mathrm{d}^2K\, \mathbf{H}(\mathbf{K}, z)\exp(i\mathbf{K}\cdot\mathbf{R}). \quad (1f)$$

Using the two Maxwell's equations and the constitutive relation,

$$\nabla\times\mathbf{E} = i\frac{\omega}{c}\mathbf{H}, \quad (2a)$$

$$\nabla\times\mathbf{H} = -i\frac{\omega}{c}\mathbf{D}, \quad (2b)$$

$$\mathbf{D}(\mathbf{r}) = \epsilon(\mathbf{r})\mathbf{E}(\mathbf{r}), \quad (2c)$$

we eliminate the z component and obtain a set of equations for the field inside each sublayer:

$$\frac{\partial E_x(\mathbf{K}, z)}{\partial z} = -i\left\{-\frac{\omega}{c}H_y(\mathbf{K}, z) + \frac{cK_x}{\omega}\frac{1}{(2\pi)^2}\int \mathrm{d}^2K' \times \epsilon^{-1}(\mathbf{K}-\mathbf{K}', z_c)[K_x'H_y(\mathbf{K}', z) - K_y'H_x(\mathbf{K}', z)]\right\}, \quad (3a)$$

$$\frac{\partial E_y(\mathbf{K}, z)}{\partial z} = -i\left\{\frac{\omega}{c}H_x(\mathbf{K}, z) + \frac{cK_y}{\omega}\frac{1}{(2\pi)^2}\int \mathrm{d}^2K' \times \epsilon^{-1}(\mathbf{K}-\mathbf{K}', z_c)[K_x'H_y(\mathbf{K}', z) - K_y'H_x(\mathbf{K}', z)]\right\}, \quad (3b)$$

$$\frac{\partial H_x(\mathbf{K}, z)}{\partial z} = -i\left[\frac{cK_xK_y}{\omega}E_x(\mathbf{K}, z) - \frac{cK_x^2}{\omega}E_y(\mathbf{K}, z) + \frac{\omega}{c}\frac{1}{(2\pi)^2}\int \mathrm{d}^2K'\,\epsilon(\mathbf{K}-\mathbf{K}', z_c)E_y(\mathbf{K}', z)\right], \quad (3c)$$

$$\frac{\partial H_y(\mathbf{K}, z)}{\partial z} = -i\left[\frac{cK_y^2}{\omega}E_x(\mathbf{K}, z) - \frac{cK_xK_y}{\omega}E_y(\mathbf{K}, z) - \frac{\omega}{c}\frac{1}{(2\pi)^2}\int \mathrm{d}^2K'\,\epsilon(\mathbf{K}-\mathbf{K}', z_c)E_x(\mathbf{K}', z)\right], \quad (3d)$$

where z_c is the z coordinate of the center of the sublayer and

$$\epsilon(\mathbf{K}-\mathbf{K}', z_c) = \int \mathrm{d}^2R\,\epsilon(\mathbf{R}, z_c)\exp[i(\mathbf{K}-\mathbf{K}')\cdot\mathbf{R}], \quad (3e)$$

$$\epsilon^{-1}(\mathbf{K}-\mathbf{K}', z_c) = \int \mathrm{d}^2R[\epsilon(\mathbf{R}, z_c)]^{-1}\exp[i(\mathbf{K}-\mathbf{K}')\cdot\mathbf{R}]. \quad (3f)$$

Equations (3) are valid over the range $z_c + \Delta z/2 \geq z \geq z_c - \Delta z/2$, where Δz is the thickness of the sublayer. This thickness can vary for different sublayers and is determined by the condition that the z dependence of the permittivity for a given sublayer can be neglected. Equations (3) are quite general, since the Fourier components of $\epsilon(\mathbf{r})$ are the only part that depends on the structure of the grating. These can be calculated easily without significant change to any program by having a routine that calculates $\epsilon(\mathbf{K}, z_c)$ and $\epsilon^{-1}(\mathbf{K}, z_c)$ for a given structure. This can be accomplished analytically or with the use of fast-Fourier-transform routines, which is the way in which we implemented the program. Equations (3) can be written concisely as

$$\frac{\partial\mathbf{A}}{\partial z} = -i\mathbf{M}\mathbf{A}, \quad (4)$$

where the column vector

$$\mathbf{A} = \begin{pmatrix} E_x(\mathbf{K}, z) \\ E_y(\mathbf{K}, z) \\ H_x(\mathbf{K}, z) \\ H_y(\mathbf{K}, z) \end{pmatrix}$$

and $\mathbf{M}$ is a square matrix obtained from Eqs. (3). Since $\mathbf{M}$ is independent of z within a given sublayer, the solution for $\mathbf{A}$ is

$$\mathbf{A}(z) = \mathbf{S}\mathbf{e}^{-i\lambda z}\mathbf{C}, \quad (5)$$

where $\mathbf{C}$ is a column vector of unknown constants, $\mathbf{e}^{-i\lambda z}$ is a diagonal matrix (λ are the eigenvalues of $\mathbf{M}$), and $\mathbf{S}$ is the matrix that diagonalizes $\mathbf{M}$ and has columns that are the eigenvectors of $\mathbf{M}$:

$$\mathbf{S}^{-1}\mathbf{M}\mathbf{S} = \Lambda\,. \tag{6}$$

The square matrix Λ is a diagonal matrix of eigenvalues λ.

Next we define a square $\mathbf{r}$ matrix that relates the tangential electric and magnetic fields on both sides of a given sublayer as follows:

$$\begin{pmatrix} \tilde{\mathbf{E}}(\mathbf{K}, z) \\ \tilde{\mathbf{E}}(\mathbf{K}, z + \Delta z) \end{pmatrix} = \mathbf{r}(\Delta z) \begin{pmatrix} \tilde{\mathbf{H}}(\mathbf{K}, z) \\ \tilde{\mathbf{H}}(\mathbf{K}, z + \Delta z) \end{pmatrix}, \tag{7}$$

where the tilde notation

$$\tilde{\mathbf{E}} = \begin{pmatrix} E_x \\ E_y \end{pmatrix}, \qquad \tilde{\mathbf{H}} = \begin{pmatrix} H_x \\ H_y \end{pmatrix}$$

signifies a column vector. The notation $\mathbf{r}(\Delta z)$ is meant to emphasize dependence on the difference in z (as shown below), even though the $\mathbf{r}$ matrix also depends on the eigenvectors and the eigenvalues associated with a given sublayer. To obtain an expression for $\mathbf{r}(\Delta z)$, we sectorize Eq. (5) and rewrite it as

$$\begin{pmatrix} \tilde{\mathbf{E}}(\mathbf{K}, z) \\ \tilde{\mathbf{H}}(\mathbf{K}, z) \end{pmatrix} = \begin{bmatrix} \mathbf{S}_{11} & \mathbf{S}_{12} \\ \mathbf{S}_{21} & \mathbf{S}_{22} \end{bmatrix} \begin{bmatrix} \mathbf{e}^{-i\lambda_1 z} & 0 \\ 0 & \mathbf{e}^{-i\lambda_2 z} \end{bmatrix} \begin{pmatrix} \mathbf{C}_1 \\ \mathbf{C}_2 \end{pmatrix}. \tag{8}$$

From Eqs. (7) and (8) we find that

$$\mathbf{r}(\Delta z) = \begin{bmatrix} \mathbf{r}_{11}(\Delta z) & \mathbf{r}_{12}(\Delta z) \\ \mathbf{r}_{21}(\Delta z) & \mathbf{r}_{22}(\Delta z) \end{bmatrix} = \begin{bmatrix} \mathbf{S}_{11} & \mathbf{S}_{12} \\ \mathbf{S}_{11}\mathbf{e}^{-i\lambda_1 \Delta z} & \mathbf{S}_{12}\mathbf{e}^{-i\lambda_2 \Delta z} \end{bmatrix} \times \begin{bmatrix} \mathbf{S}_{21} & \mathbf{S}_{22} \\ \mathbf{S}_{21}\mathbf{e}^{-i\lambda_1 \Delta z} & \mathbf{S}_{22}\mathbf{e}^{-i\lambda_2 \Delta z} \end{bmatrix}^{-1}, \tag{9}$$

which shows that, in terms of z dependence, $\mathbf{r}(\Delta z)$ depends only on Δz. Equation (9) pertains to a given sublayer, but we also assume that a global $\mathbf{R}$ matrix, analogous to the $\mathbf{r}$ matrix in Eq. (7), exists that satisfies

$$\begin{pmatrix} \tilde{\mathbf{E}}(\mathbf{K}, z_1) \\ \tilde{\mathbf{E}}(\mathbf{K}, z_2) \end{pmatrix} = \mathbf{R}(z_2 - z_1) \begin{pmatrix} \tilde{\mathbf{H}}(\mathbf{K}, z_1) \\ \tilde{\mathbf{H}}(\mathbf{K}, z_2) \end{pmatrix}, \tag{10a}$$

where

$$\mathbf{R}(z_2 - z_1) = \begin{bmatrix} \mathbf{R}_{11}(z_2 - z_1) & \mathbf{R}_{12}(z_2 - z_1) \\ \mathbf{R}_{21}(z_2 - z_1) & \mathbf{R}_{22}(z_2 - z_1) \end{bmatrix}. \tag{10b}$$

Using Eqs. (7), (8), and (10) and the fact that $\tilde{\mathbf{E}}$ and $\tilde{\mathbf{H}}$ are continuous across any interface, we obtain the following recursive relationship:

$$\mathbf{R}_{11}(z_2 + \Delta z - z_1) = \mathbf{R}_{11}(z_2 - z_1) + \mathbf{R}_{12}(z_2 - z_1)[\mathbf{r}_{11}(\Delta z) - \mathbf{R}_{22}(z_2 - z_1)]^{-1}\mathbf{R}_{21}(z_2 - z_1)\,, \tag{11a}$$

$$\mathbf{R}_{12}(z_2 + \Delta z - z_1) = -\mathbf{R}_{12}(z_2 - z_1)[\mathbf{r}_{11}(\Delta z) - \mathbf{R}_{22}(z_2 - z_1)]^{-1}\mathbf{r}_{12}(\Delta z)\,, \tag{11b}$$

$$\mathbf{R}_{21}(z_2 + \Delta z - z_1) = \mathbf{r}_{21}(\Delta z)[\mathbf{r}_{11}(\Delta z) - \mathbf{R}_{22}(z_2 - z_1)]^{-1} \times \mathbf{R}_{21}(z_2 - z_1)\,, \tag{11c}$$

$$\mathbf{R}_{22}(z_2 + \Delta z - z_1) = \mathbf{r}_{22}(\Delta z) - \mathbf{r}_{21}(\Delta z)[\mathbf{r}_{11}(\Delta z) - \mathbf{R}_{22}(z_2 - z_1)]^{-1}\mathbf{r}_{12}(\Delta z)\,. \tag{11d}$$

With Eqs. (11) we have a prescription for obtaining a global $\mathbf{R}$ matrix for any structure of interest by adding successive sublayers, where the modal expansion can be used to obtain the $\mathbf{r}$ matrix of each sublayer. To initialize the recursion relations in Eqs. (11), we see from Eqs. (7) and (10) that we may set $\mathbf{R}(\Delta z) = \mathbf{r}(\Delta z)$.

Since the $\mathbf{r}$ matrix depends on the difference in the z coordinate, the $\mathbf{R}$ matrix must depend on this difference also. In other words, the $\mathbf{R}$ matrix should be independent of where the $z = 0$ plane is defined, which means that the functional dependence on z_1 and z_2 must be $\mathbf{R}(z_2 - z_1)$. We assume this in writing down Eqs. (10), but it is not necessary in order to obtain Eqs. (11). When the structure has N identical sections, the $\mathbf{R}$ matrix that links the tangential field components at both boundaries of a given section will be identical for all the sections, since they depend only on the differences in z coordinate. We therefore need to calculate the $\mathbf{R}$ matrix for only one section, using the recursive algorithm in Eqs. (11). With this, it is a simple matter to calculate the $\mathbf{R}$ matrix for N identical sections, $\mathbf{R}_N$, by using the same recursive algorithm $N - 1$ times with the $\mathbf{R}$ matrix for a single section in place of the $\mathbf{r}$ matrix.

B. Grating Diffraction: Reflection and Transmission Coefficients

Having found the $\mathbf{R}$ matrix for a given structure, we can proceed to solve for the reflection and transmission coefficients. By definition of the global $\mathbf{R}$ matrix and with the boundary conditions, we have a relation between the substrate and the superstrate, which is

$$\begin{pmatrix} \tilde{\mathbf{E}}^t(\mathbf{K}, z_1) \\ \tilde{\mathbf{E}}^r(\mathbf{K}, z_2) + \tilde{\mathbf{E}}^{\mathrm{inc}}(\mathbf{K}^{\mathrm{inc}}, z_2) \end{pmatrix} = \mathbf{R}(z_2 - z_1) \times \begin{pmatrix} \tilde{\mathbf{H}}^t(\mathbf{K}, z_1) \\ \tilde{\mathbf{H}}^r(\mathbf{K}, z_2) + \tilde{\mathbf{H}}^{\mathrm{inc}}(\mathbf{K}^{\mathrm{inc}}, z_2) \end{pmatrix}, \tag{12}$$

where $\mathbf{K}^{\mathrm{inc}}$ is the $(\hat{x}, \hat{y})$ component of the incident-beam wave vector. Since the regions containing the reflected and transmitted fields are homogeneous, the $\tilde{\mathbf{E}}$ and $\tilde{\mathbf{H}}$ fields in Eq. (12) can be related by using Eq. (2a), which yields

$$\tilde{\mathbf{H}}(\mathbf{K}, z) = \mathbf{Z}(\mathbf{K}, p)\tilde{\mathbf{E}}(\mathbf{K}, z)\,, \tag{13}$$

where

$$\mathbf{Z}(\mathbf{K}, p) = \begin{bmatrix} -\dfrac{K_x K_y}{(\omega/c)p} & -\dfrac{p^2 + {K_y}^2}{(\omega/c)p} \\ \dfrac{p^2 + {K_x}^2}{(\omega/c)p} & \dfrac{K_x K_y}{(\omega/c)p} \end{bmatrix}. \tag{14}$$

The four quadrants of this matrix are diagonal submatrices. The $\mathbf{Z}$ matrix is evaluated in the particular medium ϵ with wave vector $\mathbf{K}$ appropriate to the substrate and superstrate media, which yields

$$\tilde{\mathbf{H}}^t(\mathbf{K}, z) = \mathbf{Z}(\mathbf{K}, -p)\tilde{\mathbf{E}}^t(\mathbf{K}, z)\,, \tag{15a}$$

$$\tilde{\mathbf{H}}^r(\mathbf{K}, z) = \mathbf{Z}(\mathbf{K}, p)\tilde{\mathbf{E}}^r(\mathbf{K}, z)\,, \tag{15b}$$

where $\mathbf{K}^{\mathrm{inc}}$ is the projection of the incident-field wave vector onto the $(\hat{x}, \hat{y})$ plane. The electric and magnetic fields of the incident field are given by $\mathbf{E}^{\mathrm{inc}}$ and $\mathbf{H}^{\mathrm{inc}}$.

Using Eqs. (15) in Eq. (12) yields

$$\begin{bmatrix} \mathbf{I} - \mathbf{R}_{11}\mathbf{Z}(\mathbf{K}, -p) & -\mathbf{R}_{12}\mathbf{Z}(\mathbf{K}, p) \\ -\mathbf{R}_{21}\mathbf{Z}(\mathbf{K}, -p) & \mathbf{I} - \mathbf{R}_{22}\mathbf{Z}(\mathbf{K}, p) \end{bmatrix} \begin{pmatrix} \mathbf{E}^t(\mathbf{K}, z_1) \\ \mathbf{E}^r(\mathbf{K}, z_2) \end{pmatrix} = \begin{bmatrix} \mathbf{0} & \mathbf{R}_{12} \\ -\mathbf{I} & \mathbf{R}_{22} \end{bmatrix} \begin{pmatrix} \mathbf{E}^{\text{inc}}(\mathbf{K}^{\text{inc}}, z_2) \\ \mathbf{H}^{\text{inc}}(\mathbf{K}^{\text{inc}}, z_2) \end{pmatrix}, \quad (16)$$

where $\mathbf{I}$ and $\mathbf{0}$ are the identity and null matrices. We can then solve Eq. (16), which yields the x and y components of the reflected and transmitted electric fields. From these results it is straightforward to obtain the diffraction efficiencies by using Eqs. (15) to calculate the magnetic fields, calculate and take the real part of the z component of the Poynting vector for the reflected and transmitted fields, and normalize with respect to the z component of the incident field.

C. Photonic Media: Dispersion Relations

The previous subsection considered diffraction of incident energy by an inhomogeneous medium, which could represent a grating. We now use the same basic formalism to examine the dispersion of energy propagating in an inhomogeneous medium. If we assume that each section is identical with period L and $N \to \infty$, we may invoke the Floquet theorem and obtain a dispersion relation. From Eq. (8) we multiply and combine the diagonal eigenvalue matrix with the column vector $\mathbf{C}$ to obtain

$$\tilde{\mathbf{E}}(\mathbf{K}, z) = \mathbf{S}_{11}\mathbf{C}_1(z) + \mathbf{S}_{12}\mathbf{C}_2(z), \quad (17a)$$

$$\tilde{\mathbf{H}}(\mathbf{K}, z) = \mathbf{S}_{21}\mathbf{C}_1(z) + \mathbf{S}_{22}\mathbf{C}_2(z). \quad (17b)$$

Because of the periodicity, the eigenvector matrix $\mathbf{S}$ and the associated eigenvalue terms (absorbed into $\mathbf{C}$) in Eqs. (17) are identical at $z = z_1$ and $z = z_1 + L$. We now use Eqs. (17) in Eqs. (10) with $z_2 = z_1 + L$ to obtain

$$\begin{aligned} \begin{pmatrix} \mathbf{C}_1(z_1 + L) \\ \mathbf{C}_2(z_1 + L) \end{pmatrix} &= \exp(iK_zL) \begin{pmatrix} \mathbf{C}_1(z_1) \\ \mathbf{C}_2(z_1) \end{pmatrix} \\ &= \begin{bmatrix} \mathbf{R}_{12}\mathbf{S}_{21} & \mathbf{R}_{12}\mathbf{S}_{22} \\ \mathbf{S}_{11} - \mathbf{R}_{22}\mathbf{S}_{21} & \mathbf{S}_{12} - \mathbf{R}_{22}\mathbf{S}_{22} \end{bmatrix}^{-1} \\ &\quad \times \begin{bmatrix} \mathbf{S}_{11} - \mathbf{R}_{11}\mathbf{S}_{21} & \mathbf{S}_{12} - \mathbf{R}_{11}\mathbf{S}_{22} \\ \mathbf{R}_{21}\mathbf{S}_{21} & \mathbf{R}_{21}\mathbf{S}_{22} \end{bmatrix} \\ &\quad \times \begin{pmatrix} \mathbf{C}_1(z_1) \\ \mathbf{C}_2(z_1) \end{pmatrix}, \end{aligned} \quad (18)$$

where K_z is the z component of the wave vector. Note that we need to calculate the $\mathbf{R}$ matrix for only one section and the eigenmatrix $\mathbf{S}$ for the initial sublayer.

We obtain the dispersion relation from Eq. (18) as follows. We assume an initial direction of propagation within the periodic medium given by the wave vector $(\mathbf{K}^{\text{inc}}, K_z)$. For a fixed value of $\mathbf{K}^{\text{inc}}$ in the $(\hat{x}, \hat{y})$ plane we can vary the wavelength, find the complex eigenvalues of the matrix in Eq. (14), look for those that have unit magnitude, equate to the scalar phase $\exp(iK_zL)$, and solve for K_z. When a particular wavelength yields a value of K_z such that $(\mathbf{K}^{\text{inc}}, K_z)$ has the desired direction of propagation, a point on the dispersion curve is found. For additional points we can then change the magnitude of $\mathbf{K}^{\text{inc}}$ and repeat the process. Over a range of wavelengths diagonalization of Eq. (18) may not yield any eigenvalues that have unit magnitude, and this implies a band gap. When eigenvalues of unit magnitude are found, half of these solutions correspond to positive values of K_z and the other half correspond to negative values of K_z. For an eigenvalue of unit magnitude obtained from Eq. (18) we use the associated eigenvector $\mathbf{C}(z_1)$ in Eqs. (17) and calculate the electric and magnetic fields. With this result we readily find the mode polarization and relative distribution of energy within each diffracted order. Note that, for a given eigenvalue, all diffracted order(s) have the same K_z.

3. NUMERICAL RESULTS

A. Diffraction from Nonabsorbing Dielectric Sinusoidal Grating

We first show a comparison of our method versus the multilayer modal method with the $\mathbf{R}$-matrix propagation of Li.[1] Both methods use the same recursive approach, but the difference lies in the way in which the modal expansion is performed. Table 1 (this is Table 3 in Li[1]) shows the diffraction efficiencies of a sinusoidal grating with $\epsilon = (2.25, 0.0)$ and period $d = 1.7\lambda$ at various heights h. The incident angle (θ, ϕ) is (30, 0). The grating is divided into 50 sublayers, and 41 diffracted orders were kept in the expansion, just as in the Li calculation. The agreement is good in general. It becomes worse as h/d becomes larger, and TE polarization agrees better than TM polarization. Li's results and ours compare very well with those of other methods (Rayleigh, integral) when applicable (see Table 3 in Li[1]).

B. Diffraction from Absorbing Metallic Sinusoidal Grating

We now compare our results for diffraction from metallic sinusoidal gratings with those given by Li[1] and Depine.[16]

Table 2 shows our results compared with those of Li (Table 4 of Li[1]), where the metallic grating has a dielectric constant $\epsilon = (-48.91, 4.2)$, angle of incidence 30°, and $d/\lambda = 1.7$. For TM polarization we choose 105 diffracted orders and 10 sublayers, and for TE polarization we choose 51 diffracted orders and 50 sublayers. Again, these values are the same number of sublayers and orders as those used by Li.[1] For the TE polarization case the comparison is good, although not as good as it is for the dielectric case. Again, when applicable, our results and Li's[1] compare well with those from alternative methods as given in Table 4 of Li's paper. However, the TM polarization comparison is quite poor, and in this case Li stated that as the number of diffracted orders or sublayers is changed, his numerical results fluctuate.

Depine[16] used the surface impedance boundary condition to extend an integral theory of perfectly conducting gratings to finite conductivity. The grating is described by dielectric constant $\epsilon = (-5.28, 1.48)$ at $\lambda = 0.55$ μm with ratios $\lambda/d = 0.5$ and $h/\lambda = 0.4$. We subdivide the sinusoidal profile into 51 sublayers and retain 83 diffracted orders. We omit TE polarization, since our results are essentially identical with those of Depine.[16] TM polarization results of efficiency versus angle of incidence are given in Fig. 1, where our

Table 1. Diffraction Efficiencies of Lossless Sinusoidal Grating

	$h/d = 0.1$		$h/d = 1.0$		$h/d = 10$		$h/d = 100$	
Order	Ours	Li's	Ours	Li's	Ours	Li's	Ours	Li's
TE polarization								
R_{-2}	0.6113(−3)	0.6109(−3)	0.3390(−2)	0.3392(−2)	0.1089(−2)	0.9572(−3)	0.1180(−2)	0.1164(−2)
R_{-1}	0.9682(−2)	0.9677(−2)	0.7626(−3)	0.7668(−3)	0.1776(−3)	0.1755(−3)	0.7734(−3)	0.7752(−3)
R_0	0.4164(−1)	0.4166(−1)	0.2031(−2)	0.2055(−2)	0.1460(−2)	0.1499(−2)	0.1003(−2)	0.1011(−2)
T_{-3}	0.6962(−5)	0.7070(−5)	0.2007(−1)	0.1994(−1)	0.3235(−2)	0.2970(−2)	0.1635(−2)	0.1653(−2)
T_{-2}	0.4640(−4)	0.4655(−4)	0.1523	0.1520	0.4924	0.4974	0.1986	0.1983
T_{-1}	0.1687(−1)	0.1677(−1)	0.4960	0.4959	0.4113	0.4111	0.7949(−1)	0.7959(−1)
T_0	0.8727	0.8727	0.2077	0.2080	0.6982(−1)	0.6750(−1)	0.6894	0.6896
T_1	0.5856(−1)	0.5852(−1)	0.1177	0.1180	0.2044(−1)	0.1838(−1)	0.2789(−1)	0.2791(−1)
TM polarization								
R_{-2}	0.7730(−3)	0.7761(−3)	0.1644(−2)	0.1730(−2)	0.3159(−4)	0.5851(−4)	0.3012(−3)	0.1965(−2)
R_{-1}	0.9086(−2)	0.9124(−2)	0.7107(−3)	0.6672(−3)	0.2239(−6)	0.1217(−5)	0.4110(−5)	0.2101(−3)
R_0	0.1485(−1)	0.1495(−1)	0.1726(−3)	0.1866(−3)	0.1023(−3)	0.1046(−3)	0.1603(−3)	0.2456(−3)
T_{-3}	0.4687(−5)	0.7888(−5)	0.1131(−1)	0.1282(−1)	0.4376(−3)	0.6417(−3)	0.1569(−2)	0.4140(−2)
T_{-2}	0.6059(−4)	0.5918(−4)	0.2126	0.2134	0.1905	0.1869	0.1463	0.1383
T_{-1}	0.1486(−1)	0.1485(−1)	0.4637	0.4616	0.2812	0.2757	0.9248(−1)	0.8550(−1)
T_0	0.9359	0.9354	0.1886	0.1836	0.5185	0.5261	0.7340	0.7503
T_1	0.2447(−1)	0.2485(−1)	0.1214	0.1260	0.9277(−2)	0.1045(−1)	0.2516(−1)	0.1936(−1)

Table 2. Diffraction Efficiencies of Lossy Sinusoidal Grating

	$h/d = 0.1$		$h/d = 1.0$		$h/d = 10$		$h/d = 100$	
Order	Ours	Li's	Ours	Li's	Ours	Li's	Ours	Li's
TE polarization								
R_{-2}	0.0116	0.0116	0.4152	0.4135	0.1885	0.1993	0.0558	0.0733
R_{-1}	0.2066	0.2067	0.3338	0.3353	0.1353	0.1372	0.0233	0.0202
R_0	0.7604	0.7602	0.2010	0.2018	0.3086	0.3010	0.0225	0.0171
TM polarization								
R_{-2}	0.0258	0.0279	0.0274	0.1264	0.0160	0.0494		0.0057
R_{-1}	0.2564	0.2784	0.0664	0.0603	0.0078	0.3307		0.0164
R_0	0.6131	0.6519	0.2146	0.6609	0.0315	0.1618		0.0747

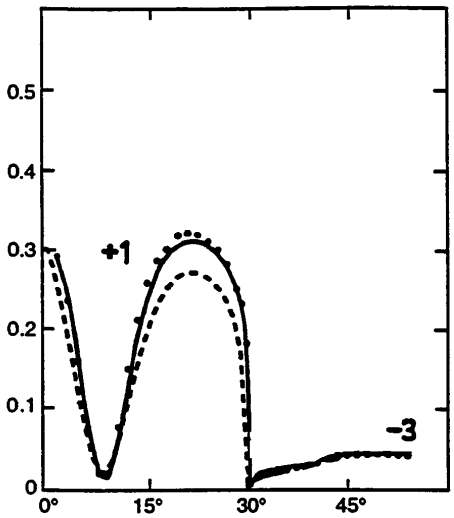

Fig. 1. TM polarization diffraction efficiency versus angle of incidence from a lossy sinusoidal grating. We compare our +1 and −3 diffracted order results (dashed curves) with those of Depine[16] (solid curve). The dielectric constant is $\epsilon = (-5.28, 1.48)$, $h/\lambda = 0.4$, and $d/\lambda = 2.0$.

results (dashed curves) are compared with those of Depine (solid curve). We see that our results generally agree, with some disagreement in the neighborhood of 20°.

C. Infinite- and Finite-Thickness Photonic Crystal

Next we calculate the transmission through a two-dimensional photonic crystal of finite depth consisting of infinitely long cylinders arranged in a square array. In our notation the cylinder axis is along the y direction. The lattice constant is 1.87 mm, and the radius of the cylinder is 0.37 mm. The index of refraction, n, of the cylinder is 2.98. Robertson *et al.*[15] have measured the transmission through such a structure that is seven rows deep (see Fig. 2) using the coherent microwave transient spectroscopy technique. Since the structure has seven rows of cylinders (seven identical sections), we need to calculate the **R** matrix for only the first section (marked by the top pair of dashed lines in Fig. 2). Once this **R** matrix is obtained, we can use it in conjunction with the recursive method to obtain the global $R_{N=7}$ for all seven sections as discussed above. To calculate the **R** matrix for one section, we subdivide it into $M + 2$ sublayers (M sublayers for the cylinder plus one sublayer each for the region above and below the cylinder). In Fig. 3 we show the transmission as a function of the frequency for TE and TM polarization. The dashed–dotted curves are the transmission for normal incidence resulting from our calculation, and the dots are experimental data.[15] Since the coherent microwave transient spectroscopy technique is a pulse experiment, the frequency content will be weighted differently. The weight is ob-

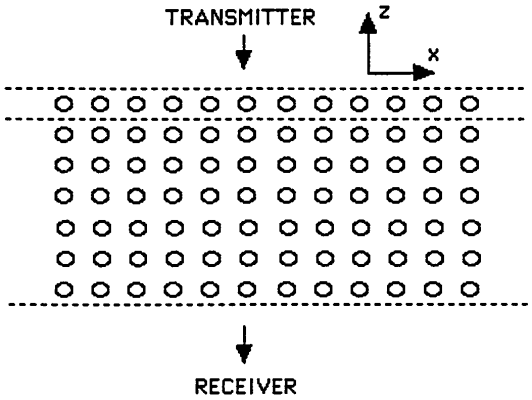

Fig. 2. Schematic of a square array of infinitely long cylinders seven rows deep. The cylinders are infinitely long in the y direction and infinitely periodic in the x direction.

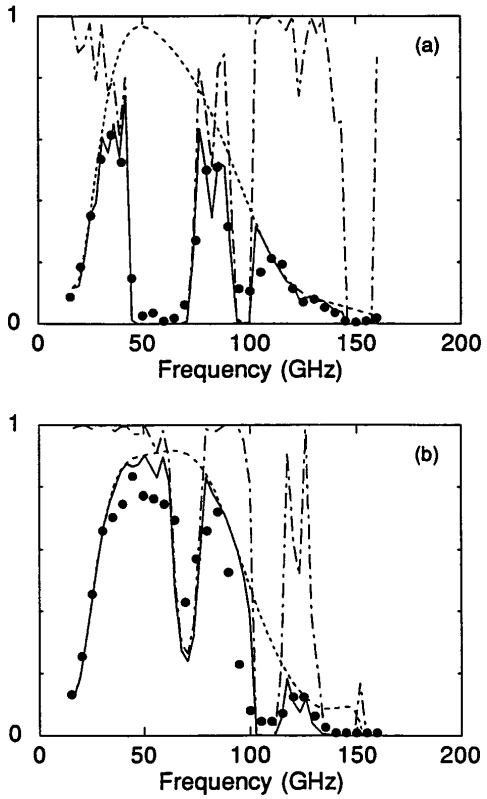

Fig. 3. Transmission versus frequency of a photonic crystal array consisting of seven rows of infinitely long cylinders (see Fig. 2). The dashed–dotted curves show our results for transmission at normal incidence. The dashed curves are the experimental reference curve, and the solid curves are the product of the reference and the calculated transmission. The dots are measured data, and the polarization is (a) parallel and (b) perpendicular to the cylinder axes.

tained by measuring the transmission in the absence of the sample (this is called the reference curve in Ref. 15). The dashed curves are our ninth-order polynomial fit to the reference curve. The solid curves are the product of the calculated transmission and the reference curve. The result agrees quite well with the experimental data. The fact that the experimental cylinder is not infinitely long and that the number of cylinders is also not infinite in the x direction (i.e., the structure is not periodic in the x–y plane) may account for some of the discrepancies between theory and experiment. The number of diffracted orders kept in the calculation is 51, and $M = 50$. We also increased the number of diffracted orders kept to 101 and M to 100, but the spectra did not change.

We can let the cylinder array described above be infinitely extended in the z direction, and, following the procedure outlined in Subsection 2.C, we can calculate the dispersion relations. Our results agree with those of Robertson *et al.*[15] Alternatively, we also note that from our transmission data we can obtain the phase shift ϕ as the wave propagates through the crystal of thickness L. From the phase shift we can obtain the effective refractive index $n(\omega) = 1 + (\phi c/\omega L)$ and derive the dispersion curve $k = \omega n(\omega)/c$, as was done by Robertson *et al.*[15] in their experiment.

4. CONCLUSIONS

We have presented a coupled-mode theory for calculation of diffraction of incident energy by inhomogeneous media, including gratings, and dispersion of electromagnetic energy propagating in photonic media. The method is quite general, in that complex three-dimensional periodic structures can be treated. It is straightforward to treat structures that are infinitely periodic in the x–y plane and of arbitrary structure in the z direction by dividing this structure into sublayers. This includes a method to repeat the arbitrary structure, whole structures at a time, to form a finitely periodic structure in the z direction. This latter property is a feature of the recursive numerical algorithm, which can be very significant in terms of computational efficiency.

We have used a recursive, **R**-matrix, approach that is much more stable than a transfer, **T**-matrix, approach. We calculate the recursive matrices quite simply by finding the eigenvalues and the eigenvectors of a matrix. Our results compare favorably with those in the published literature for diffraction (reflection and transmission) and photonic dispersion. We find that for reflection and transmission diffraction from sinusoidal gratings, TE polarization agrees very well with published results. For TM polarization we find increasing disagreement with some published results as the grating depth increases.

We have also calculated transmission diffraction from a seven-layer-deep square array of dielectric cylinders. Our results agree very well with measured data. Also, numerical results for photonic dispersion from an infinitely deep square arrangement of infinitely long dielectric cylinders are calculated by applying the Floquet theorem and agree with published results.

ACKNOWLEDGMENTS

The work of P. Tran was supported by the U.S. Office of Naval Research code 1121RS and a U.S. Office of Naval Technology/American Society for Engineering Education Fellowship. Support of J. M. Elson was provided by U.S. Navy In-House Independent Research funds.

REFERENCES

1. L. Li, "Multilayer modal method for diffraction gratings of arbitrary profile, depth, and permittivity," J. Opt. Soc. Am. A **10,** 2581–2591 (1993).

2. D. J. Zvijac and J. C. Light, "**R**-matrix theory for collinear chemical reactions," Chem. Phys. **12,** 237–251 (1976); J. C. Light and R. B. Walker, "An **R**-matrix approach to the solution of coupled equations for atom–molecule reactive scattering," J. Chem. Phys. **65,** 4272–4282 (1976).
3. L. C. Botten, M. S. Craig, R. C. Mcphedran, J. L. Adams, and J. R. Andrewartha, "The dielectric lamellar diffraction grating," Opt. Acta **28,** 413–428 (1981); L. C. Botten, M. S. Craig, R. C. Mcphedran, J. L. Adams, and J. R. Andrewartha, "The finitely conducting lamellar diffraction grating," Opt. Acta **28,** 1087–1102 (1981).
4. E. Yablonovitch, "Inhibited spontaneous emission in solid-state physics and electronics," Phys. Rev. Lett. **58,** 2059–2062 (1987).
5. S. John, "Strong localization of photons in certain disordered dielectric super lattices," Phys. Rev. Lett. **58,** 2486–2489 (1987).
6. S. John and J. Wang, "Quantum electrodynamics near a photonic band gap: photon bound states and dressed atoms," Phys. Rev. Lett. **64,** 2418–2421 (1990).
7. K. M. Leung and Y. F. Liu, "Full vector wave calculation of photonic band structures in face-centered-cubic dielectric media," Phys. Rev. Lett. **65,** 2646–2649 (1990).
8. Z. Zhang and S. Satpathy, "Electromagnetic wave propagation in periodic structures: Bloch wave solutions of Maxwell's equations," Phys. Rev. Lett. **65,** 2650–2653 (1990).
9. K. M. Ho, C. T. Chan, and C. M. Soukoulis, "Existence of a photonic gap in periodic dielectric structure," Phys. Rev. Lett. **65,** 3152–3155 (1990).
10. K. M. Leung and Y. Qiu, "Multiple scattering calculation of the two-dimensional photonic band structure," Phys. Rev. B **48,** 7767–7771 (1993).
11. X. Wang, X. G. Zhang, Q. Yu, and B. N. Harmon, "Multiple scattering theory for electromagnetic waves," Phys. Rev. B **47,** 4161–4167 (1992).
12. J. B. Pendry and A. MacKinnon, "Calculations of photon dispersion relations," Phys. Rev. Lett. **69,** 2772–2775 (1992).
13. N. F. Johnson and P. M. Hui, "Theory of propagation of scalar waves in periodic and disordered composite structures," Phys. Rev. B **48,** 10118–10123 (1993).
14. J. B. Pendry, "Photonic band structures," J. Mod. Opt. **41,** 209–230 (1994).
15. W. M. Robertson, G. Arjavalingam, R. D. Meade, K. D. Brommer, A. M. Rappe, and J. D. Joannopoulos, "Measurement of photonic band structure in a two-dimensional periodic dielectric array," Phys. Rev. Lett. **68,** 2023–2026 (1992).
16. R. A. Depine, "Perfectly conducting diffraction grating formalisms extended to good conductors via the surface impedance boundary condition," Appl. Opt. **26,** 2348–2354 (1987).